IAWA Journal, Vol. 25 (1), 2004: 79–90

X-RAY MICROANALYSIS USING THIN SECTIONS OF PRESERVATIVE-TREATED WOOD
Relationship of wood anatomical features to the distribution of copper

Hiroshi Matsunaga[1], Junji Matsumura[2] & Kazuyuki Oda[2]

SUMMARY

The objective of this study was to understand the micro-distribution of a copper-based preservative in wood in connection with anatomical morphology and to consider the fixation of copper in wood. Bulk specimens and semi-ultra thin sections (0.5 μm) obtained from Japanese cedar (*Cryptomeria japonica*) were treated with a CuAz preservative solution. After fixation of the solution in wood components, SEM-EDXA (Scanning Electron Microscope equipped with an Energy Dispersive X-ray Analyzer) was used to investigate the micro-distribution of copper. The use of semi-ultra thin sections improved characteristic X-ray spatial resolution and made it possible to analyze the micro-distribution of copper. In both earlywood and latewood of the sapwood, copper was more abundant in the compound middle lamella than in the secondary wall and concentrated in the tori. Copper was most concentrated as crystalline deposits in longitudinal parecnhyma cells. Semi-quantitative analysis revealed the copper amount to increase in this order: secondary wall in tracheids < middle lamellae < membrane of half-bordered pits < tori in tracheid pits < deposits in longitudinal parenchyma cells. These different concentrations may indicate significant interactions between the amine-copper complex in CuAz and chemical constituents of wood.

Key words: SEM-EDXA, CuAz, micro-distribution, parenchyma, torus, *Cryptomeria japonica*.

INTRODUCTION

Wood preservatives need a high ability of fixation to provide effective protection. The interaction and the fixation between the components of preservatives and wood are not well understood.

It is important to understand the bulk flow pathways of aqueous preservatives solutions in wood for assessing preservative impregnation. Preservative micro-distribution can also affect performance. For example, certain anatomical features may affect the distribution of preservatives, even if the solution sufficiently penetrates the wood. In order to understand the distribution of preservatives in wood, it is necessary to consider the interactions between preservatives and wood components, in relation to wood anatomy.

1) Forestry and Forest Products Research Institute, Wood Preservation Laboratory, P.O. Box 16, Tsukuba 305-8687, Japan [E-mail: mhiroshi@ffpri.affrc.go.jp].
2) Department of Forest and Forest Products Sciences, Faculty of Agriculture, Kyushu University, Fukuoka 812-8581, Japan.

The aim of this study was to clarify the differences in the distribution of copper in Japanese cedar (*Cryptomeria japonica*) sapwood treated with a CuAz preservative solution. SEM-EDXA (Scanning Electron Microscope equipped with an Energy Dispersive X-ray Analyzer) technique was used to understand CuAz fixation to wood. This enabled us to analyze the micro-distribution of copper in wood and where and how the interactions between preservatives and wood components occur.

MATERIALS AND METHODS

Wood samples

Bulk specimens were used to analyze preservative distribution in relation to anatomical features under low magnification, while semi-ultra thin sections were used to study the micro-distribution and the amount of copper concentration in wood under high magnification (Fig. 1).

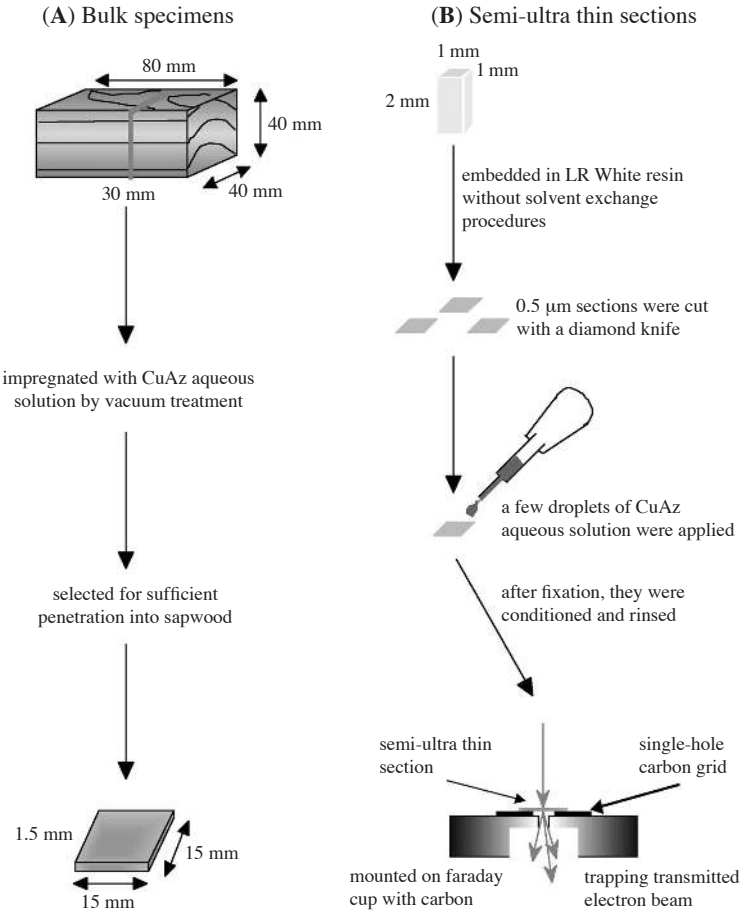

Fig. 1. Diagram on bulk specimens and semi-ultra thin sections.

Bulk specimens — Five air-dried Japanese cedar (*Cryptomeria japonica* D. Don) sapwood blocks (80 (L) × 40 (R) × 40 (T) mm) were immersed in a CuAz aqueous solution diluted 30-fold with distilled water and then placed in a vacuum at 4 kPa for 30 minutes. The specimens were removed from the vacuum and remained in the solution an additional 20 minutes at regular atmospheric pressure. The undiluted CuAz aqueous solution includes copper oxide (11.3% w/w), boric acid (9% w/w) and tebuconazole (0.45% w/w) as active ingredients, as well as monoethanolamine and a surface active agent as dissolution agents. Uptake (grams per cubic centimeter) was calculated by dividing the difference in weight before and after impregnation by the sample volume. Mean uptake of five samples was 0.64 g/cm^3 (standard deviation: 0.028). The treated blocks were conditioned at room temperature for 3 weeks. After conditioning they were cut and found to be colored moss green throughout, which confirmed that the solution sufficiently penetrated the blocks. At 30 mm from the surface of these treated blocks, 20 bulk specimens (15 × 15 × 1.5 mm) were prepared for SEM-EDXA. To expose the radial surface, specimens were split; to expose the transverse surface, they were dry-cut with a sliding microtome. Bulk specimens were attached to carbon specimen stubs using double-sided carbon-cello tape and carbon-coated in a vacuum evaporator (JEOL JEC520).

Semi-ultra thin sections — Semi-ultra thin sections were prepared to clarify the degree of CuAz concentration in the micro regions in wood. When an electron beam is used to irradiate wood, the characteristic X-ray spatial resolution spreads by the μm order (Matsunaga et al. 2000, 2001a, 2001b), namely, over the cell wall width. Figure 2A shows a Monte Carlo simulation of electron trajectories through a bulk sample. There is poor X-ray spatial resolution and this method cannot provide information on the distribution and concentration of preservatives within secondary walls, middle lamellae, bordered pits, etc. In order to investigate the distribution of preservatives in the micro regions, semi-ultra thin sections were prepared to improve the characteristic X-ray spatial resolution below ~0.5 μm (Saka & Thomas 1982; Ryan 1986; Ryan & Draysdale 1988; Williams & Carter 1996; Matsunaga et al. 2002). Figure 2B shows a Monte Carlo

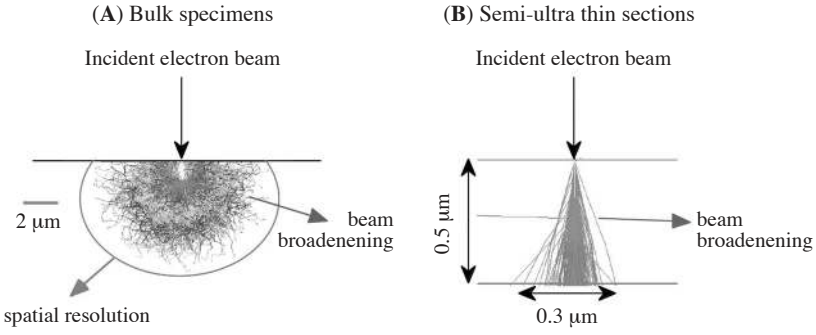

Presented by Dr. M. Watanabe at Lehigh Univ. and partly recognized

Fig. 2. Monte Carlo simulation of electron trajectories between bulk and thin specimens. – Bulk specimens give a poor X-ray spatial resolution, whereas thin sections improve it.

simulation of electron trajectories through a thin section. Compared with a bulk sample, the total beam-specimen interaction volume is decreased so that a higher X-ray spatial resolution is obtained. The use of semi-ultra thin sections would permit analysis of the secondary walls, middle lamellae, and bordered pits as a separate entity.

Hundred small sticks (2 (L) × 1 (R) × 1 (T) mm) from Japanese cedar (*Cryptomeria japonica*) sapwood blocks were embedded in LR White resin by vacuum immersion without solvent exchange procedures (Matsunaga et al. 2002). Semi-ultra thin sections (0.5 μm, transverse section) were cut with a diamond knife using a Leica RM2045 microtome. CuAz treatment was performed by dropping CuAz aqueous solution over the sections (Fig. 1B). After fixation of the CuAz preservatives and wood components, the sections were rinsed with distilled water in order to remove unreacted preservatives and placed over a 0.5 mm single-hole carbon grid and carbon-coated to prevent charging. The carbon grid with sections was then placed on a specimen grid holder made of carbon within which a Faraday cup was fabricated. Specimens were held in the air so that the electron beam transmitted through sections never irradiated the specimen holder with carbon and continuum X-ray from the holder was eliminated and minimized (Matsunaga et al. 2002) (Fig. 1). The preliminary SEM-EDXA analysis indicated that no elements were detected in the LR White resin present in the cell lumens.

SEM-EDXA technique

The bulk specimens were examined in a JEOL JSM-5600LV scanning electron microscope (SEM) equipped with a JEOL JED-2140 energy dispersive X-ray analyzer (EDXA) which only detects elements above sodium in the periodic table are detected. The conditions used in this study were accelerating voltage 15 kV; illuminating current 5 nA; working distance 20 mm; takeoff angle 30°; tilt angle 0°; dead time 15–20%; dwell time (digital map) 0.1 msec/point; pixels 512 × 512; elemental peaks detected Cu-Kα; window width 7.96–8.14 keV. Backscattered electron images (BEI) that produced both specimen shapes and contrast by atomic number were mainly observed.

For digital mapping images, the X-ray intensity on each pixel indicated different hues of color using the software furnished with EDXA. A warmer hue represented the higher X-ray intensity, that is, high concentration, with the white areas representing the highest concentration.

For semi-ultra thin sections, conditions for EDXA were the same as for bulk specimens except the accelerating voltage was 30 kV and illuminating current 1.5 nA. The X-ray intensities of copper were measured by 100 live second point analysis. The peak intensity (characteristic X-ray) is proportional to wt.% (Tsuchiya 1998). On the other hand, the continuum X-ray (background) intensity is proportional to the mass inside the irradiated volume (Matsunaga et al. 2001a, 2001b, 2002). The ratio P/B (peak/background) was used as an index of the relative quantity of copper.

Spatial resolution

When the electron beam was used to irradiate the specimens, electrons diffusely penetrated the specimen (Fig. 2A). X-ray spatial resolution depends upon the region of electron broadening. For a bulk sample it is assumed that all inelastic scatterings of

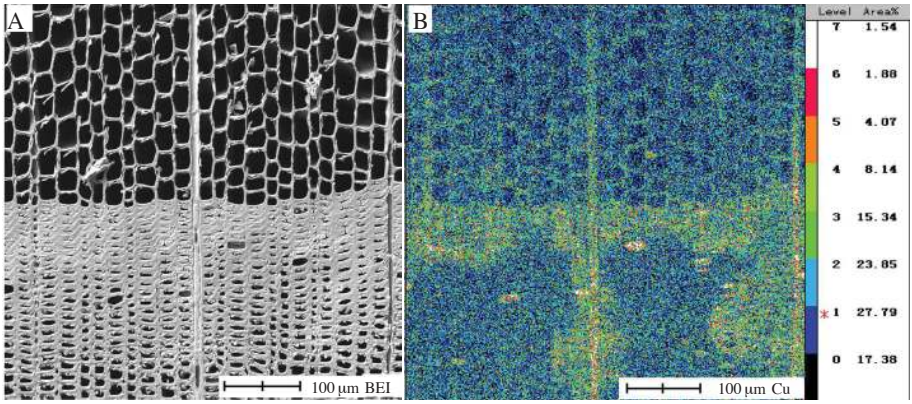

Fig. 3 SEM-EDXA color mapping images for a transverse section of *Cryptomeria japonica* sapwood impregnated by vacuum treatment with CuAz aqueous solution. — A: backscattered electron image; B: Cu-Kα X-ray image. The brighter the color, the higher the concentration. Copper is concentrated in latewood near the growth ring boundary, ray parenchyma cells and longitudinal parenchyma cells.

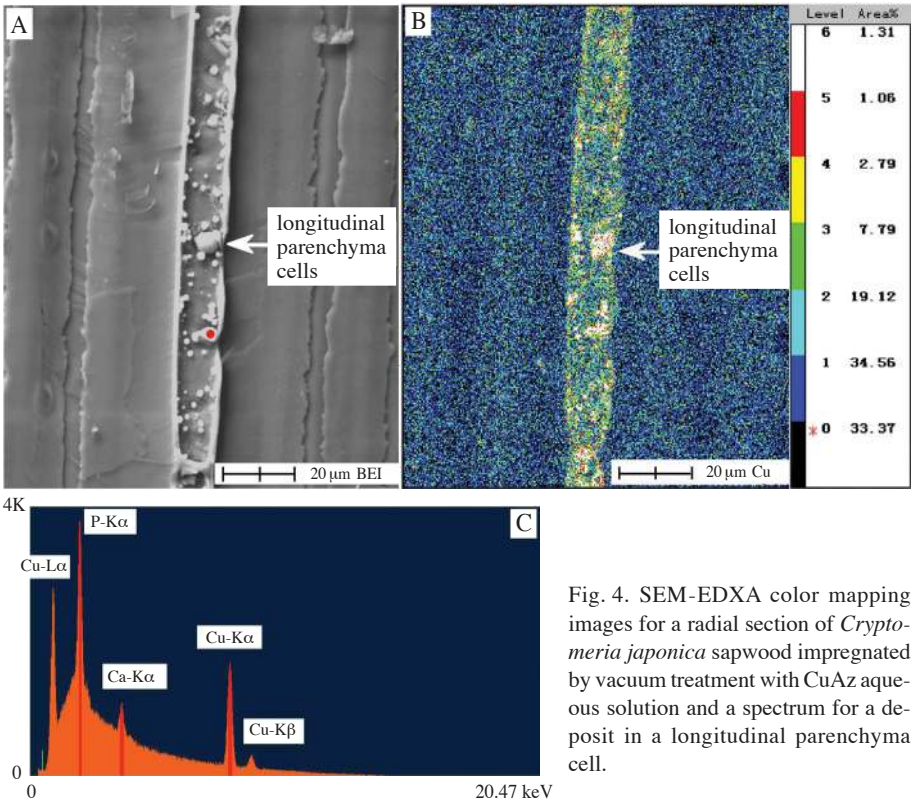

Fig. 4. SEM-EDXA color mapping images for a radial section of *Cryptomeria japonica* sapwood impregnated by vacuum treatment with CuAz aqueous solution and a spectrum for a deposit in a longitudinal parenchyma cell.

A: backscattered electron image; B: Cu-Kα X-ray image; C: spectrum for a deposit in a longitudinal parenchyma cell. The brighter the color, the higher the concentration. Copper is concentrated in longitudinal parenchyma cells and distributed in the shape of crystalline deposits. Point analysis location (red point) is shown in Fig. 4A.

the incident electron beam are absorbed. The approximate value of the depth (Z_m in μm) of the analyzed region was given by Castaing (1960) as follows:

$$Z_m = 0.033 \left(V_o^{1.7} - V_k^{1.7}\right)^{A/\rho Z}$$

where V_o is accelerating voltage (kV), V_k the critical excitation potential associated with a particular X-ray line (minimum energy necessary for exciting the X-ray line) in kV, A is the mean atomic mass of the bombarded point, Z is its mean atomic number, and ρ the local density of the specimen (g/cm^3).

It can be assumed that the total diameter of the analyzed region (d in μm) is equal to

$$d = d_o + Z_m$$

where d_o (μm) is the diameter of the electron probe and Z_m the maximum effective range. In this study it was calculated that the Cu-Kα spatial resolution was within 4–6 μm.

For thin sections the calculation for spatial resolution is different from that used for bulk samples (Castaing 1960; Kanaya & Okayama 1972; Goldstein et al. 1992; Williams & Carter 1996) (Fig. 2B).

Assuming that each electron only undergoes one elastic scattering event as it traverses a thin section, the amount that the beam spreads on its way through the section is defined as follows (Reed 1982):

$$b = 7.21 \times 10^5 \times \frac{Z}{E_o} \left(\frac{\rho}{A}\right)^{0.5} t^{1.5}$$

where b is beam spreading (cm), Z its mean atomic number, E_o incident electron energy (eV), ρ density of the specimen (g/cm^3), A mean atomic weight and t specimen thickness (cm).

This definition encompasses 90% of the electrons emerging from a thin section, so it is consistent with the definition of the incident beam diameter (d). The total region (analyzed region) where the incident beam traverses the thin section approximates a cone. The beam diameter (Rmax) after traversing the thin section is:

$$R\text{max} = \left(d_p^2 + b^2\right)^{0.5}$$

where dp is the incident beam diameter (cm).

Although it can be considered that the X-ray generates anywhere the beam traverses the thin section, it is well known that the spatial resolution derived from this equation is larger than in actual experiments. Michael et al. (1990) proposed that the definition of R (spatial resolution) should be modified so as not to present the worst case (given by the exit beam diameter) but to define R midway through the thin section.

$$R = \left(d_p + R\text{max}\right) / 2$$

This equation is the formal definition of the X-ray spatial resolution on thin sections. In the present study it was calculated that the spatial resolution was within 0.3 μm, which is good enough to analyze each micro region as isolated.

RESULTS

Copper distribution (Bulk specimen)

Figure 3 shows a digital color map of a transverse section of sapwood treated with CuAz. Figure 3A indicates a backscattered electron image. Figure 3B illustrates a Cu-Kα X-ray image and represents the concentration differences in color, that is, the warmer the color, the higher the Cu-Kα X-ray intensity, with white representing the highest. Although specimens were selected in which the CuAz aqueous solution sufficiently penetrated throughout, copper was more abundant in latewood tracheids near growth ring boundaries, longitudinal parenchyma cells and ray parenchyma cells.

Copper distribution of longitudinal parenchyma cells, where copper was especially heavily concentrated, was investigated in radial sections (Fig. 4). Figure 4A indicates a backscattered electron image (BEI) and Figure 4B an Cu-Kα X-ray image. In Figure 4A, BEI shows that the contrast in the whole of the longitudinal parenchyma cell, especially the deposits, was emphasized more than in adjacent tracheids, that is, there is a heavy element with a large atomic number. The Cu-Kα X-ray image (Fig. 4B) indicates that the copper was detected in the longitudinal parenchyma cell and many crystalline deposits were fringed with copper. Point analysis detected phosphorus and calcium in the deposits in the longitudinal parenchyma cells (Fig. 4C). It can be presumed that copper forms complexes with the contents of the longitudinal parenchyma cells. These results indicae that parenchyma cells were rich in copper.

Copper micro-distribution (semi-ultra thin section)

Tracheids — The Cu-Kα line profile (Fig. 5) indicates that copper is more abundant in the compound middle lamellae than in the secondary wall in tracheids. There were no elements in the cell lumen resin, indicating that the CuAz solution did not react with resin used for embedding. These images also indicate a high Cu-Kα X-ray spatial resolution corresponding to the secondary electron image.

Point analyses were carried out to clarify the localization of copper in the cell wall (Fig. 6). Compared with bulk specimens (Fig. 4C), the continuum X-ray (background) intensity in each spectrum was generally low, especially on the low energy side. This means that the incident electron beam was well transmitted and little inelastic scattering occurred when compared with the bulk specimens. Point analyses indicated that the level of Cu-Kα was higher in the compound middle lamellae than in the secondary walls. Similar results were obtained in earlywood.

Analysis of thin sections revealed that copper was more abundant in the compound middle lamella and cell corner than in the secondary cell wall. There are several reports (Chou et al. 1973; Ryan & Draysdale 1988; Lee et al. 1992) that chromium, copper and arsenic were more abundant in the compound middle lamella than in the secondary wall in wood treated with chromated-copper-arsenate (CCA). Copper distribution in CuAz treated wood resembled that with CCA.

Bordered pits

The bordered pits were particularly important regions for copper distribution. Figure 7 shows an example of a bordered pit in latewood treated with CuAz. Figure 7A represents a secondary electron image and Figure 7B an image obtained by superposi-

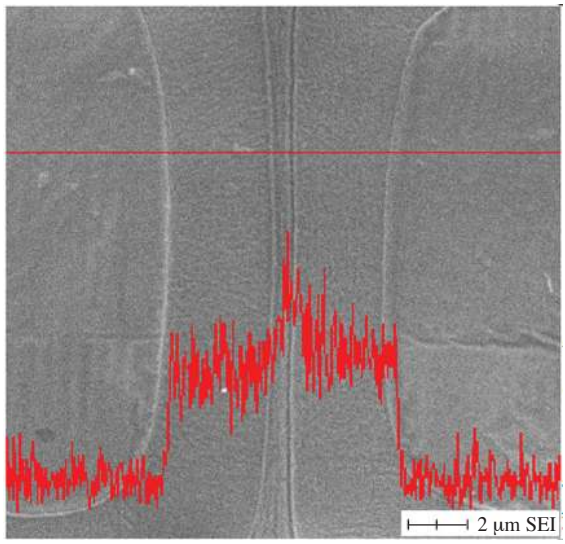

Fig. 5. SEM-EDXA image obtained by superpositioning of a secondary electron image and Cu-Kα line profile for a semi-ultra thin section of *Cryptomeria japonica* sapwood treated with CuAz (latewood, transverse section). – Copper is more concentrated in the compound middle lamellae than in the secondary wall in tracheids.

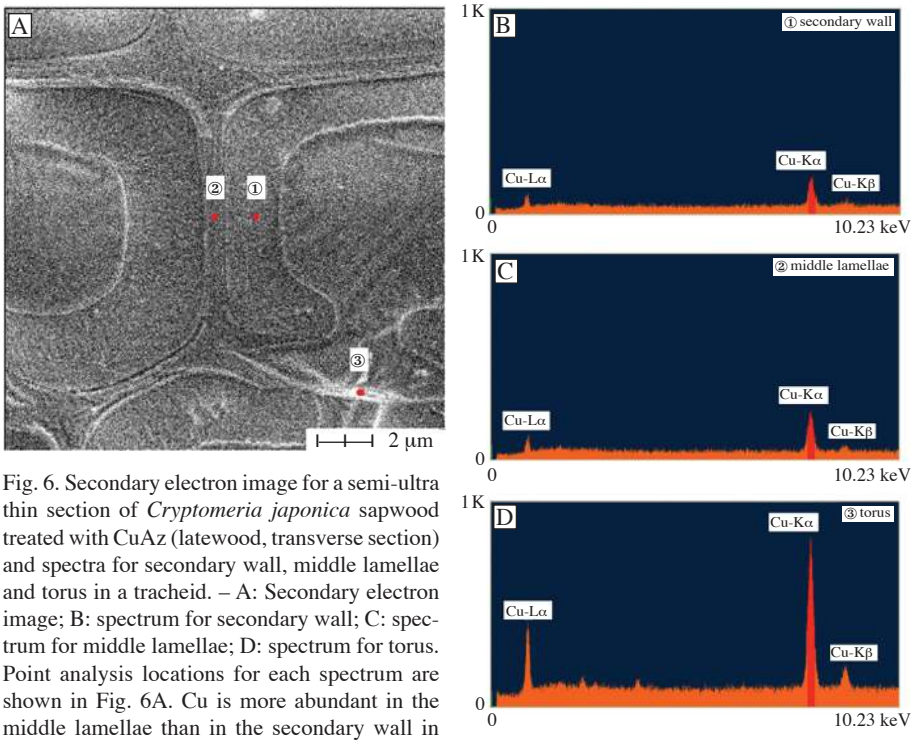

Fig. 6. Secondary electron image for a semi-ultra thin section of *Cryptomeria japonica* sapwood treated with CuAz (latewood, transverse section) and spectra for secondary wall, middle lamellae and torus in a tracheid. – A: Secondary electron image; B: spectrum for secondary wall; C: spectrum for middle lamellae; D: spectrum for torus. Point analysis locations for each spectrum are shown in Fig. 6A. Cu is more abundant in the middle lamellae than in the secondary wall in tracheids.

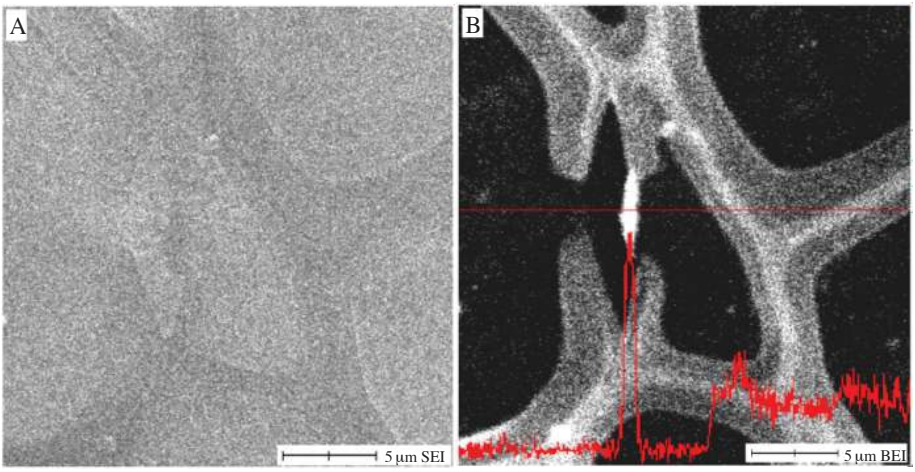

Fig. 7. Secondary electron image and backscattered electron image of a semi-ultra thin section of *Cryptomeria japonica* sapwood treated with CuAz (latewood, transverse section). — A: secondary electron image; B: image obtained by superpositioning of the backscattered electron image and Cu-Kα X-ray line profile. Copper is more abundant in the torus, the compound middle lamellae including the cell corner, and secondary wall.

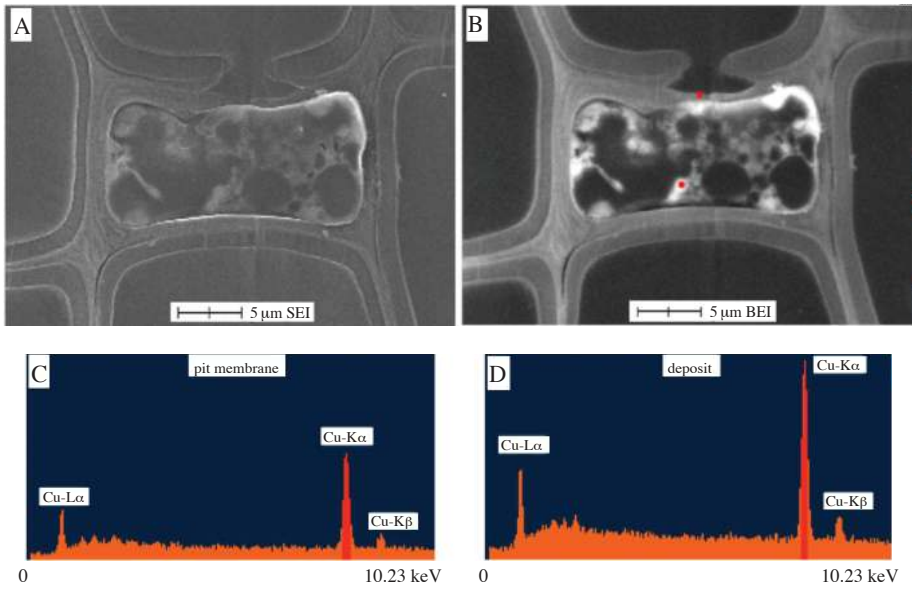

Fig. 8. Secondary electron image and backscattered electron image of a longitudinal parenchyma cell in a semi-ultra thin section of *Cryptomeria japonica* sapwood treated with CuAz (latewood, transverse section) and spectra for a half-bordered pit membrane and deposit in the cell. — A: secondary electron image; B: backscattered electron image; C: spectrum for half-bordered pit membrane; D: spectrum for a deposit in the longitudinal parenchyma cell. Point analysis locations are shown in Fig. 8B. Copper is localized in many crystalline deposits in the longitudinal parenchyma cell.

tioning the backscattered electron image and Cu-Kα X-ray line profile. Backscattered electron imaging emphasizes the contrast of the compound middle lamella, including cell corner and torus, compared with secondary wall. Backscattered electrons increase with increasing atomic number and this is the basis for atomic number contrast (also called compositional contrast of Z contrast). Figure 7B indicates that the atomic number increases from secondary wall in tracheid to the compound middle lamella to torus. The Cu-Kα X-ray line profile showed that copper levels were also higher in this order. Point analysis (Fig. 6C) indicated that the intensity of the Cu-Kα signal in the torus was also greater than in the cell wall. Similar results were obtained in earlywood (Matsunaga et al. 2002). These results suggest that tori play an important role in preservative fixation.

Longitudinal parenchyma cell

Longitudinal parenchyma cells contained the greatest amount of copper. Figure 8 gives an example of latewood longitudinal parenchyma cell treated with CuAz. Figure 8A represents a secondary electron image and Figure 8B a backscattered electron image. The secondary electron image showed that the deposits were in the longitudinal parenchyma cells. Backscattered electrons (Fig. 8B) emphasize a contrast of the contents of the longitudinal parenchyma cell when compared to the cell wall. From point analyses (Fig. 8C & D), copper was extremely rich and many crystalline deposits were fringed with copper. Pit membranes of half-bordered pits had the same high level of copper concentration as the torus. Copper was mostly localized in deposits in longitudinal parenchyma cells.

DISCUSSION

With Japanese cedar sapwood, the results of bulk analysis revealed that the copper concentration was uneven, although the aqueous solution penetrated the sapwood specimen entirely. With semi-ultra thin sections, the degree of CuAz concentration was clarified and it was found that the degree of copper fixation is related to wood anatomy.

Figure 9 indicates the peak to background (P/B) ratio as the relative quantity of copper in each region as shown in semi-ultra thin sections. From semi-quantitative analysis, the content of copper increased in this order: secondary wall in tracheids < middle lamellae < half-bordered pit membranes < tori in tracheids < deposits in longitudinal parenchyma cells.

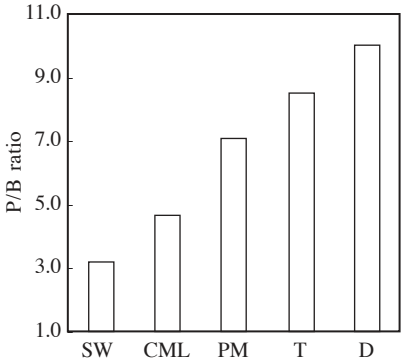

Fig. 9. Comparison of P/B ratios of copper in the secondary wall, compound middle lamellae, half-bordered pit membrane, torus, and the deposit in the longitudinal parenchyma cells in *Cryptomeria japonica* sapwood treated with CuAz. — SW: secondary wall; CML: compound middle lamellae; PM: half-bordered pit membrane; T: torus; D: deposit in longitudinal parenchyma cells. Point analysis locations are shown in Fig. 6A and Fig. 8B.

The CuAz aqueous solution includes monoethanolamine and a surface active agent as a dissolution agent. Stable amine-copper complexes are formed in aqueous solution (Thomason & Pasek 1997). Copper fixation is believed to be initiated by the neutralization of acidic groups in wood by the amine (Jiang & Ruddick 1999; Zhang & Kamdem 2000; Lucas & Ruddick 2002). In the case of CuAz, the amine-copper interacts with carboxylic groups in hemicellulose and phenolic hydroxyl groups in lignin to form copper-amine-wood complexes.

Compound middle lamellae are generally rich in lignin with lignin and hemicellulose accounting for more than 90% of this zone. The elevated lignin levels may have caused the greater copper concentration in the compound middle lamellae than in the secondary wall.

On the other hand, tori of pit membranes in sapwood contain pectic substances in addition to cellulose and hemicellulose (Imamura et al. 1974; Meyer 1974; Morishita et al. 1986; Ohkoshi et al. 1987). Pectic acids consist of galacturonic acid units that also have many carboxylic groups which may help to explain the more extensive copper concentration in tori than in cell wall.

Parenchyma in sapwood are alive and contain polysaccharide (e.g. starch) and protoplasm. In the case of CuAz, it can be assumed that it is easy for copper-amine complexes to fix to acid polysaccharide contents in parenchyma tissues.

CONCLUSION

Use of the SEM-EDXA technique precisely described a relationship between anatomy and copper concentration. The following conclusions were reached:

1. Copper was more abundant in the middle lamella than in the secondary wall in both earlywood and latewood.
2. Copper was concentrated in tori of tracheids and half-bordered pit membranes.
3. In longitudinal parenchyma cells many crystalline deposits were fringed with copper complexes.
4. From semi-quantitative analysis, the relative quantity of copper increased in the order of: secondary wall in tracheids < middle lamellae < half-bordered pit membrane < tori in tracheids < deposits in longitudinal parenchyma cells.

We conclude that these different concentrations indicate predominant interactions between the amine-copper complex and chemical constituents of wood.

ACKNOWLEDGEMENTS

We thank Kyushu Wood Industry Ltd. for providing the CuAz aqueous solution. A part of this study was carried out in cooperation with the Kazato Research Foundation in Japan.

REFERENCES

Castaing, R. 1960. Electron probe microanalysis. Advances in electronics and electron physics: 317–386. Academic Press.

Chou, C.K., J.A. Chandlar, R.D. Preston & R. Ayer. 1973. Microdistribution of metal elements in wood impregnated with a copper-chrome-arsenic preservative as determined by analytical electron microscopy. Wood Sci. Technol. 7: 151–160.

Goldstein, J.I., D.E. Newbury, P. Echlin, D.C. Joy, A.D. Romig Jr, C.E. Lyman, C.E Fiori & E. Lifshin. 1992. Scanning electron microscopy and X-ray microanalysis. 2nd Ed.: 79–90 Plenum Press, New York.

Imamura, Y., H. Harada & H. Saiki. 1974. Embedding substances of pit membranes in softwood tracheids and their degradation by enzymes. Wood Sci. Technol. 8: 243–254.

Jiang, X. & J.N.R. Ruddick. 1999. A comparison of leaching resistance of diammine-copper complexes and copper carbonate precipitated wood. Internat. Res. Group on Wood Preserv., Document No. IRG/WP99-20160.

Kanaya, K. & S. Okayama. 1972. Penetration and energy-loss theory of electrons in solid targets. J. Phys. D.: Appl. Phys. 5: 43–58.

Lee, J-S., I. Furukawa & T. Sakuno. 1992. Microdistribution of elements in wood after pre-treatment with chitosan and impregnation with chrome-copper-arsenic preservative. Mokuzai Gakkaishi 38: 186–192.

Lucas, N. & J.N.R. Ruddick. 2002. Determination of amine to copper ratio remaining in wood after leaching. Internat. Res. Group on Wood Preserv., Document No. IRG/WP02-30285.

Matsunaga, H., J. Matsumura, A. Noguchi & K. Oda. 2000. Distribution of inorganic elements in wood impregnated with preservative solutions I – Visualization of inorganic element distribution in wood by SEM-EDXA. Mokuzai Gakkaishi 46: 368–374.

Matsunaga, H., J. Matsumura & K. Oda. 2001a. Distribution of inorganic elements in wood impregnated with preservative solutions II – Effect of anatomical characteristics on microdistribution of preservatives in Cryptomeria japonica sapwood. Mokuzai Gakkaishi 47: 383–388.

Matsunaga, H., J. Matsumura & K. Oda. 2001b. Visualization of inorganic element distribution in preservative treated wood by SEM-EDXA. Internat. Res. Group on Wood Preserv., Document No. IRG/WP01-40208.

Matsunaga, H., J. Matsumura., K. Oda & Y. Takechi. 2002. Microdistribution of copper in Cryptomeria japonica sapwood fixed with CuAz preservative. Mokuzai Gakkaishi 38: 199–204.

Meyer, R.W. 1974. Effect of enzyme treatment on bordered-pit ultrastructure, permeability and toughness of the sapwood of three western conifers. Wood Sci. 6: 220–230.

Michael, J.R., D.B. Williams, C.F. Klein & R. Ayer. 1990. The measurement and calculation of the X-ray spatial resolution obtained in the analytical electron microscope. J. Microscopy 160: 41–53.

Morishita, S., M. Ohkoshi., K. Nakato & T. Sadoh. 1986. Destroying obstacles in the fluid flow through softwoods with pectolytic enzymes. Mokuzai Gakkaishi 32: 401–408.

Ohkoshi, M., M. Tokuda & T. Sadoh. 1987. Increase of permeability of sugi by degrading bordered pit membranes with enzymes. Mokuzai Gakkaishi 33: 347–357.

Reed, S.J.B. 1982. The single-scattering model and spatial resolution in X-ray analysis of thin foils. Ultramicroscopy 7: 405–410.

Ryan, K.G. 1986. Preparation techniques for X-ray analysis in the transmission electron microscope of wood treated with copper-chrome-arsenate. Mater. Org. 21: 223–234.

Ryan, K.G. & J.A. Draysdale. 1988. X-ray analysis of copper cromium and arsenic within the cell walls of treated hardwoods – New evidence against the microdistribution theory. J. Inst. Wood Sci. 11: 108–113.

Saka, S & R.J. Thomas. 1982. Evaluation of the quantitative assay of lignin distribution by SEM-EDXA-technique. Wood Sci. Technol. 16: 1–18.

Thomason, S.M. & E.A. Pasek. 1997. Amine copper reaction with wood components: acidity versus copper adsorption. Internat. Res. Group on Wood Preserv., Document No. IRG/WP97-30161.

Tsuchiya, Y. 1998. Electron probe micro analyzer. Maruzen, Tokyo [In Japanese].

Williams, D.B. & C.B. Carter. 1996. Transmission electron microscopy: 623–635. Plenum Press, New York.

Zhang, J. & D.P. Kamdem. 2000. FTIR characterization of copper ethanolamine-wood interaction for wood preservation. Holzforschung 54: 119–122.